CHAPTER – 4

SOFTWARE IMPLEMENTATION OF ALGORITHM FOR RDC USING ANGLE TRACKING OBSERVER (ATO) TECHNIQUE

CHAPTER – 4

SOFTWARE IMPLEMENTATION OF ALGORITHM FOR RDC USING ANGLE TRACKING OBSERVER TECHNIQUE

4.1 INTRODUCTION

From the theory of control system, a well-designed observer tries to minimize its estimation error at every calculation. As Arctangent algorithm is an open loop method, the difference between the actual angle and the measured rotor angle of the resolver using this method is very high and gives large amount of error.

ATO based RDC is a form of tracking analog to digital converter that derives digital angle information from SIN and COS modulated resolver signals. This algorithm compares the resolver output signal values with their corresponding estimations and performs the conversion using a feedback loop by minimizing the error between the rotor shaft angle and the estimated angle. The advantage of ATO algorithm compared to the Arctangent algorithm is that it yields smooth and accurate estimations of both rotor angle and speed. The block diagram of RDC using ATO algorithm is shown in Figure 4.1.

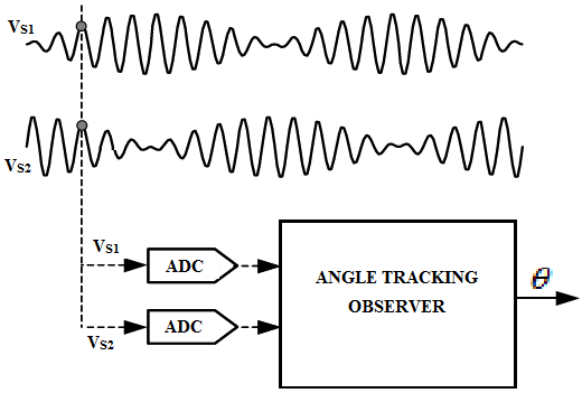

Figure 4.1 Angle extraction using angle tracking observer

4.2 MATHEMATICAL MODEL OF ATO BASED RDC

The structure of RDC using ATO algorithm is shown in Figure 4.2. The two outputs of the resolver are applied as input to the COS and SIN multipliers. These multipliers incorporate SIN and COS lookup tables and functions as multiplying digital to analog converters. Initially, the current state of the up/down counter is assumed and it is a digital number representing a trial angle, ϕ. The converter seeks to adjust the digital angle, ϕ, continuously to become equal to and to track rotor shaft angle, θ.

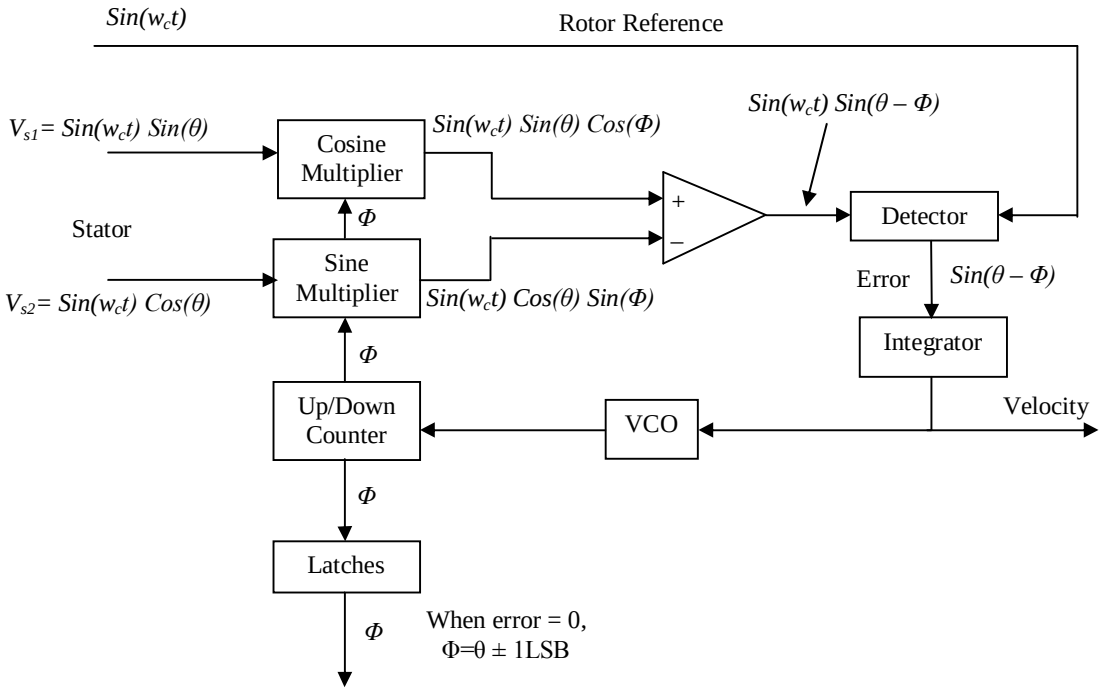

Figure 4.2 Structure of ATO based Resolver to Digital Converter

The stator output signals of the resolver are expressed as in equation (3.6) and the estimated digital angle ϕ is applied to COS multiplier, and its COS value is multiplied with V_{s1} to produce the term

$$\alpha\, ASin(w_c t)\, Sin(\theta)\, Cos(\phi) \qquad (4.1)$$

The same digital angle ϕ is applied as input to the SIN multiplier and multiplied with V_{s2} to produce the term

$$\alpha\, ASin(w_c t)\, Cos(\theta) Sin(\phi) \qquad (4.2)$$

The two signals in equation (4.1) and (4.2) are subtracted from each other with an error amplifier to yield an AC error signal of the form

$$\alpha\, ASin(w_c t)\left[Sin(\theta) Cos(\phi) - Cos(\theta) Sin(\phi)\right] \qquad (4.3)$$

The error calculation is based on the simple trigonometric identity and equation (4.3) can be reduces to

$$\alpha\, ASin(w_c t)\left[Sin(\theta - \phi)\right] \qquad (4.4)$$

This error signal is demodulated using a synchronous detector with the resolver rotor reference signal. This error signal also drives the tracking loop. This results in a DC error signal proportional to $Sin(\theta - \phi)$. There are two integrators in the tracking loop, one integrator is an analogue integrator and the second is combination of the Voltage Controlled Oscillator (VCO) and the counter. With the use of two integrators the smoothing capability of ATO algorithm is more than Arctangent algorithm. If the error is zero then the counter digital output matches with the rotor shaft angle.

$$Sin\,(\theta - \phi) \rightarrow 0 \qquad (4.5)$$

as per the Taylor approximation around zero, the equation (4.5) becomes

$$Sin(\theta - \phi) \approx (\theta - \phi) \quad for\, |\theta - \phi| << 1 \qquad (4.6)$$

when this is achieved, then as

$$(\theta - \phi) \rightarrow 0 \qquad (4.7)$$

and therefore

$$\theta = \phi \qquad (4.8)$$

to within one count. Hence, the counter's digital angle output ϕ represents the rotor angle θ. The latches enable this data to be transferred externally without interrupting the loop's tracking. The input to the VCO equals to the angular velocity.

This circuit is equivalent to a Type-II servo loop because it has two integrators. One is the counter, which accumulates pulses; the other is the integrator at the output of the detector. In a Type-II servo loop with a constant rotational velocity input, the output digital word continuously follows or tracks the input without needing externally derived convert commands and with no steady state phase lag between the digital output word and actual shaft angle. An error signal appears only during periods of acceleration or deceleration.

Because the tracking converter doubly integrates its error signal, the device offers a high degree of noise immunity (12 dB per octave roll off). The net area under any given noise spike produces an error. However, typical inductively coupled noise spikes have equal positive and negative going waveforms. When integrated, this results in a zero net error signal. The resulting noise immunity, combined with the converter's insensitivity to voltage drops. Noise rejection is further enhanced by the detector's rejection of any signal not at the reference frequency, such as wideband noise.

4.3 METHODOLOGY

The block diagram of the proposed software based resolver to digital converter based on ATO algorithm was implemented in MATLAB® SIMULINK® and is shown in Figure 4.3. The designed RDC system is an ideal system and is developed based on the theory of ATO algorithm.

The main blocks of ATO based RDC, as in Figure 4.3 are

a) Resolver System
b) Cosine and Sin multipliers
c) Product modulators
d) Synchronous demodulator
e) Continuous Time VCO
f) Counter

The MATLAB® SIMULINK® model contains a resolver system with a square wave excitation source as input and the amplitude modulated sine and cosine output signals. The resolver transformation constant is chosen as one for the simulation. So the amplitude of the resolver output signals is same as the amplitude of the excitation signal. There are two product modulators in the model. The first product modulator takes the inputs as the SIN output signal of the resolver and COS signal of the estimated angle and it gives the eq. (4.1). The eq. (4.2) is the output signal from the second product modulator with the input signals as the COS output signal of the resolver and the SIN signal of the estimated angle. The outputs of the two product modulators are applied to a summer to generate eq. (4.4). The output of the summer, as in eq. (4.4) contains the excitation signal as one of the product term.

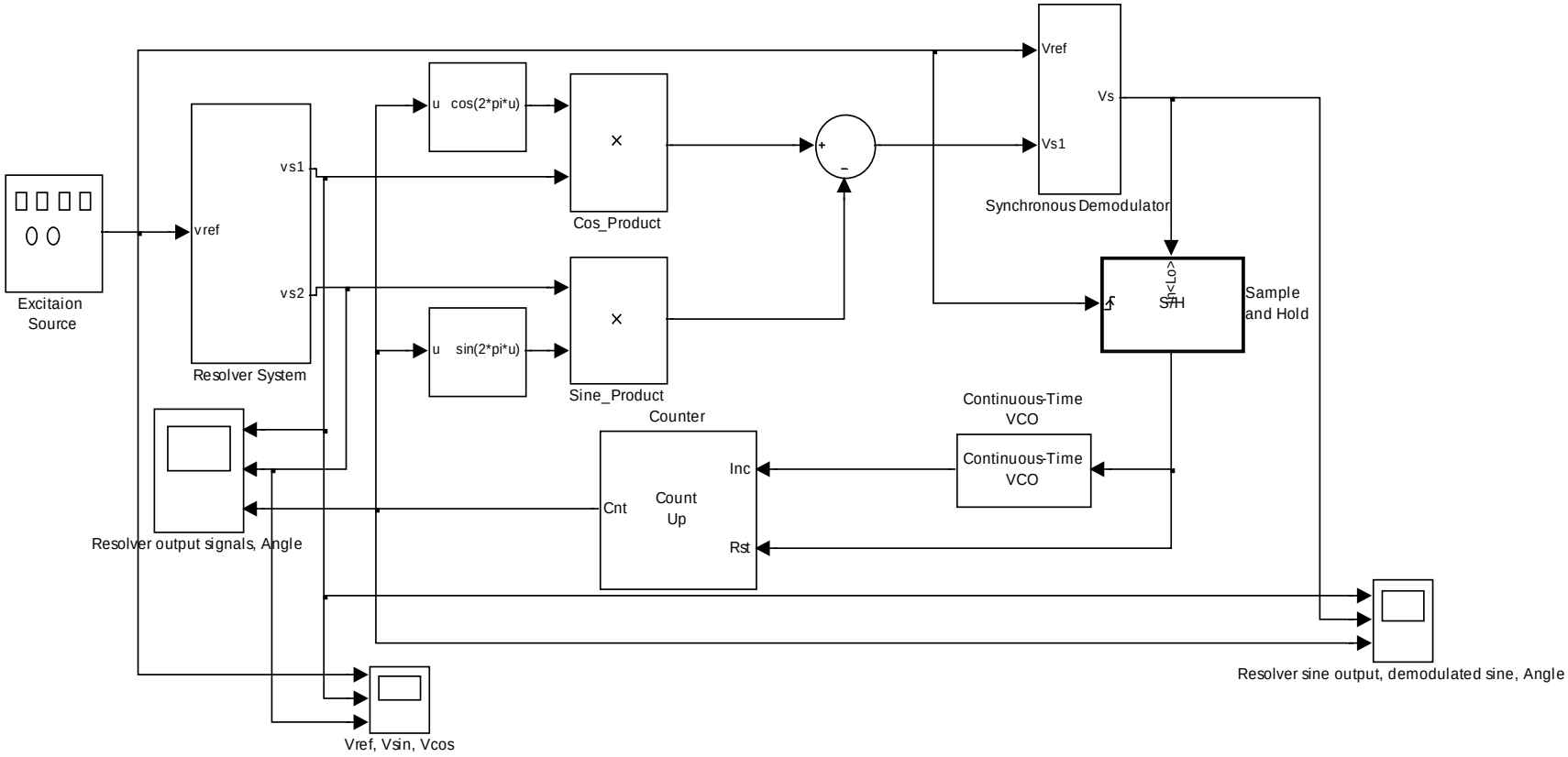

Figure 4.3 MATLAB® SIMULINK® model of RDC using ATO algorithm

The excitation signal at the output of the summer is removed using the synchronous demodulator. The synchronous demodulator block consists of a product modulator followed by a low pass filter. The output of the summer and the excitation signal are given as inputs to the product modulator. The output of the product modulator contains the higher frequency terms and lower frequency terms and is passed through low pass filter to eliminate higher frequency term i.e. excitation signal. The low pass filter is designed with a higher cut-off frequency that is equals to rotor shaft frequency. So the low pass filter removes the excitation signal frequencies and it gives only rotor signal frequency. The magnitude and phase response of designed low pass filter are shown in Figure 4.4.

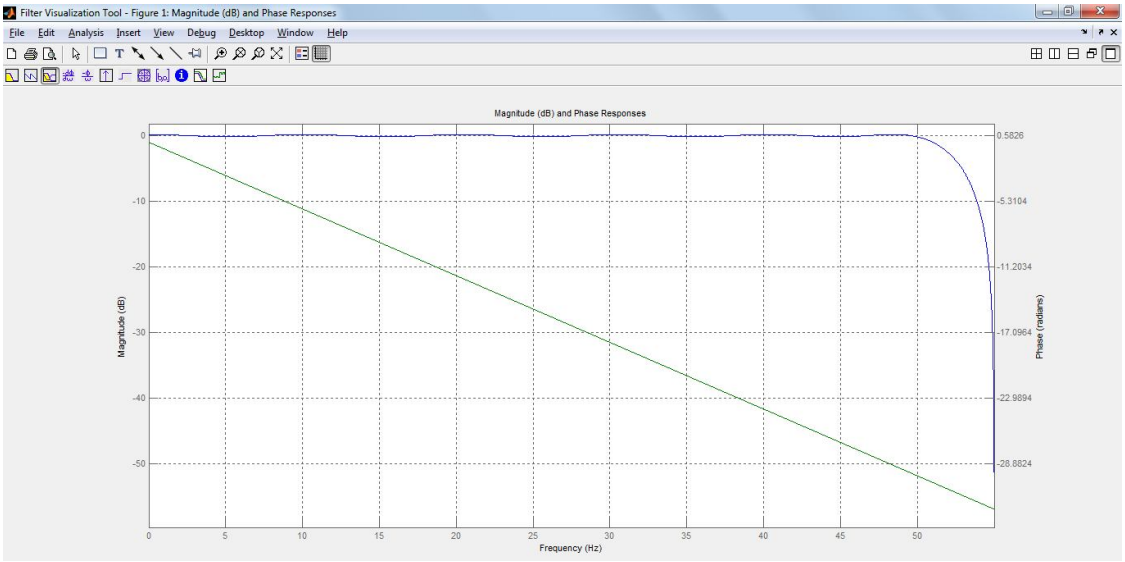

Figure 4.4 Magnitude and phase response of Low pass filter

The output of the synchronous demodulator, as in eq. (4.5) is used to measure the rotor shaft angle of the resolver. This signal is sampled at the zero crossings of the excitation signal to measure the envelope of the demodulated signal. The sampled envelope is applied to continuous VCO and counter to measure the rotor angle.

4.4 RESULTS AND DISCUSSIONS

The effectiveness of ATO algorithm based RDC model is verified using computer simulations by measuring the rotor shaft angles at different rotor speeds. The resolver is excited with a square wave excitation source of amplitude 1 Volt and 5 kHz with a sampling frequency of 100 kHz. The simulation parameters of MATLAB® SIMULINK® are same as in Table 3.1.

Case (i): When the resolver rotor speed is 300 rpm

The simulation results of the proposed RDC model when the rotor shaft speed is 300 rpm are shown from Figure 4.5 to Figure 4.7. Figure 4.5 shows the excitation signal to the resolver with amplitude of 1Volt and a frequency of 5 kHz, resolver modulated SIN and COS output signals with an amplitude of 1 Volt and a frequency of 5 Hz.

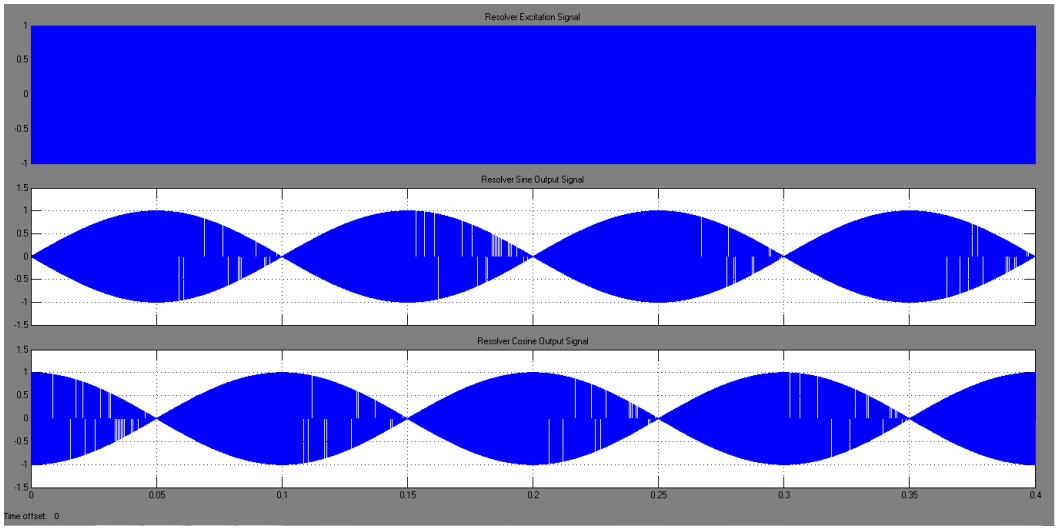

Figure 4.5 Square wave excitation signal, SIN and COS outputs of the resolver

Figure 4.6 shows the input and output signals of the synchronous demodulator. The input to the synchronous demodulator is the combination of the rotor speed and excitation signal. This excitation signal is removed using the synchronous

demodulator. The resolver SIN, COS output signals and measured rotor shaft angle are shown in Figure 4.7.

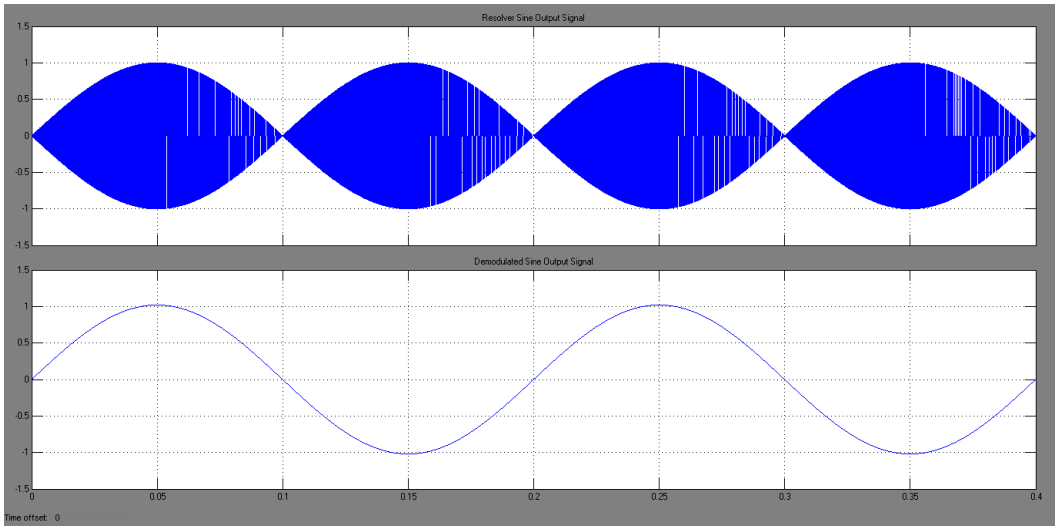

Figure 4.6 SIN output, demodulated SIN, COS output and demodulated COS signals

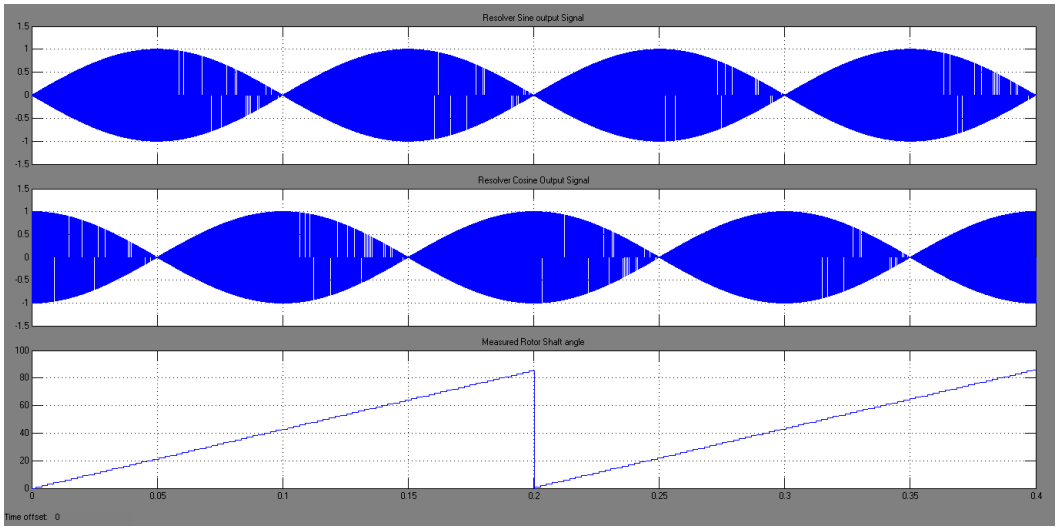

Figure 4.7 SIN, COS modulated signals of resolver and measured rotor shaft angle

Case (ii): When the resolver rotor speed is 600 rpm

The simulation results from Figure 4.8 to Figure 4.10, shows when the rotor speed is 600 rpm i.e. 10 Hz. Figure 4.8 shows resolver excitation signal of 1 Volt amplitude with a frequency of 5 kHz, resolver modulated SIN and COS output signals. The input and demodulated output of synchronous demodulator are shown in Figure 4.9. In Figure 4.10, the top trace is resolver modulated SIN output signal, middle trace is resolver modulated COS output signal and the last trace is the rotor shaft angle.

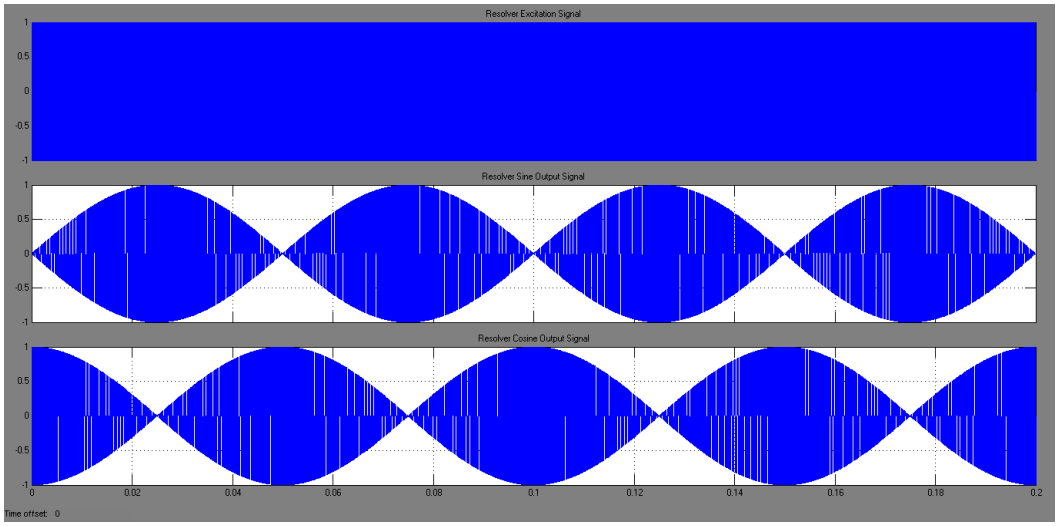

Figure 4.8 Square wave excitation signal, SIN and COS outputs of the resolver

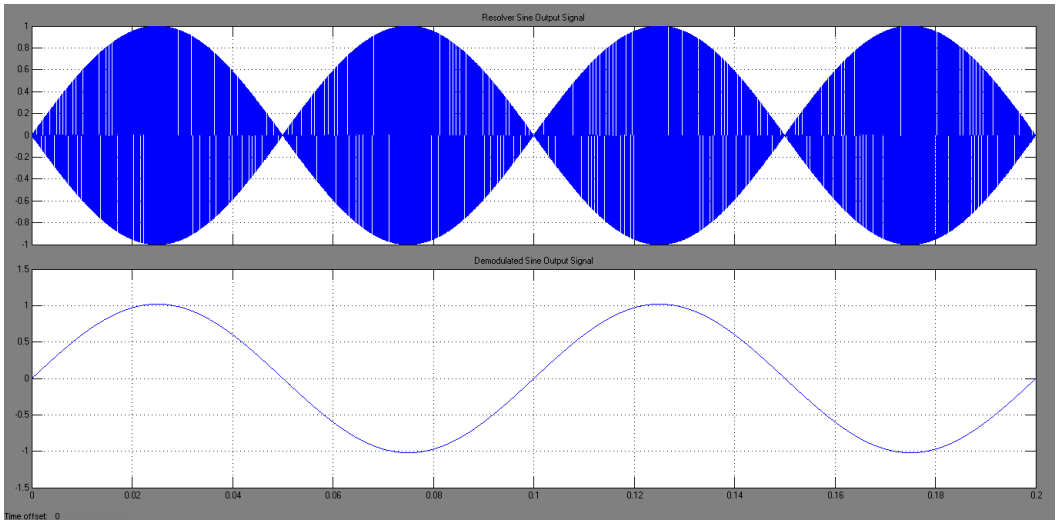

Figure 4.9 SIN output, demodulated SIN, COS output and demodulated COS signals

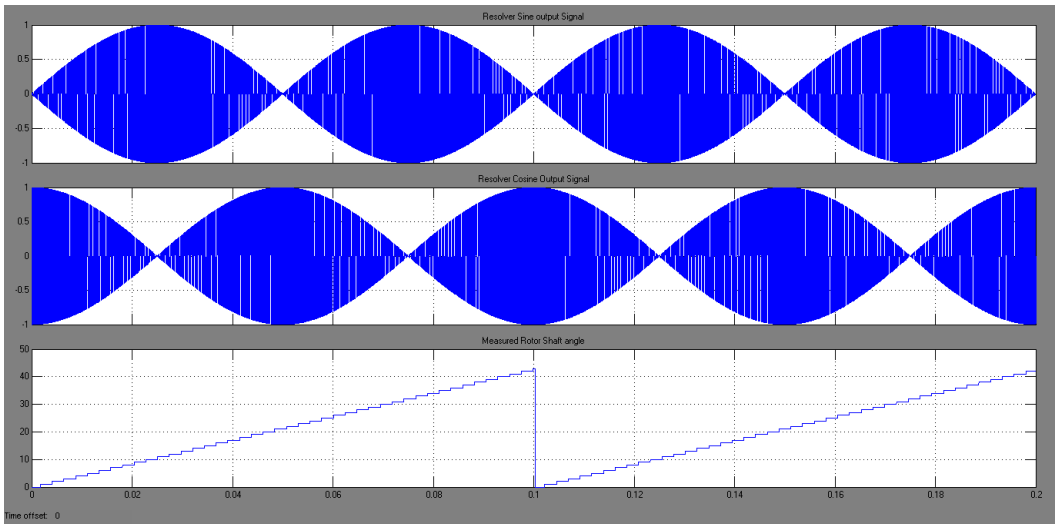

Figure 4.10 SIN, COS modulated signals of resolver and measured rotor shaft angle

Case (iii): When the resolver rotor speed is 3000 rpm

Figure 4.11 to Figure 4.13 shows the simulation results of the proposed RDC model when the rotor speed is 3000 rpm. The resolver is excited with 1 Volt amplitude and a frequency of 5 kHz. Figure 4.11 shows the resolver excitation signal and the modulated SIN and COS output signals of the resolver. The input signal to the synchronous detector and demodulated signal are shown in Figure 4.12. The modulated outputs of the resolver and measured rotor angle are shown in Figure 4.13.

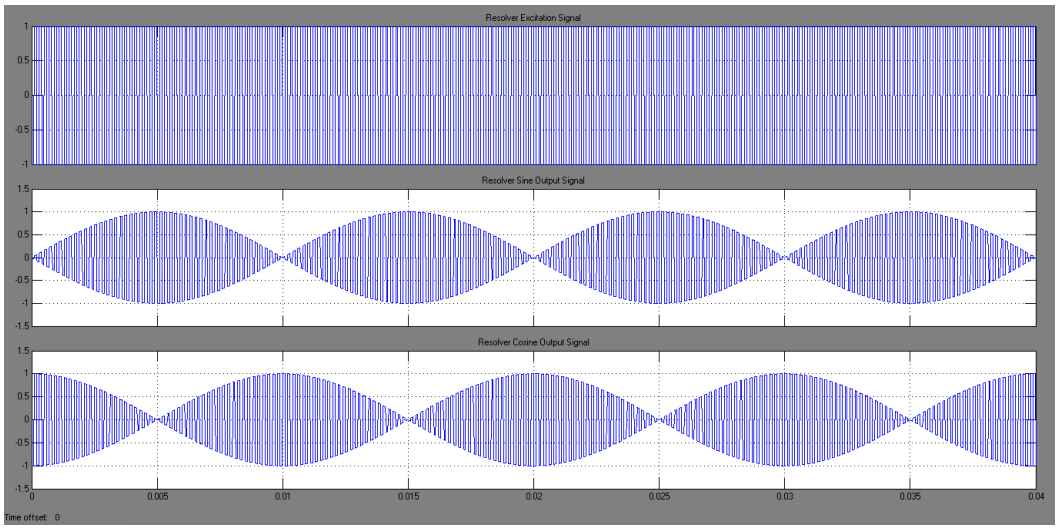

Figure 4.11 Square wave excitation signal, SIN and COS outputs of the resolver

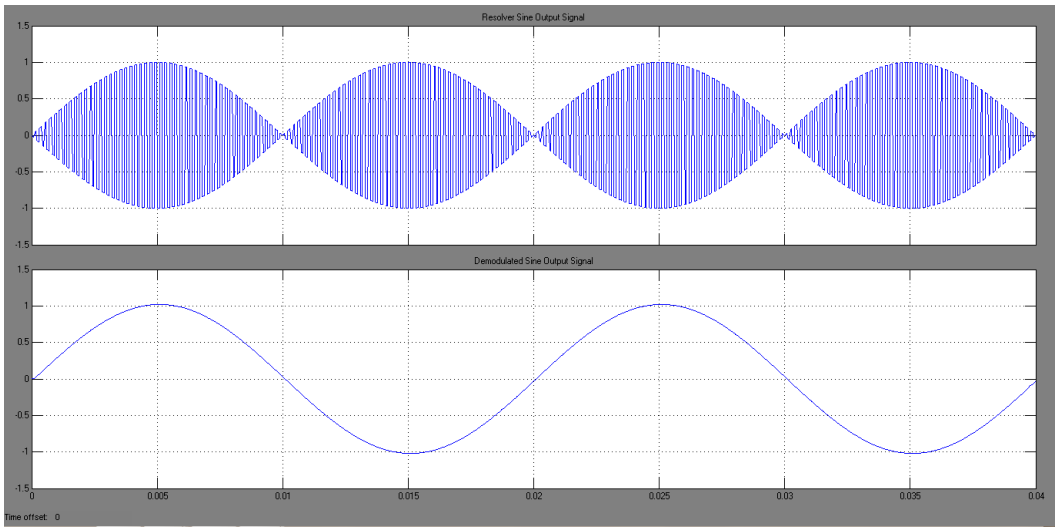

Figure 4.12 SIN output, demodulated SIN, COS output and demodulated COS signals

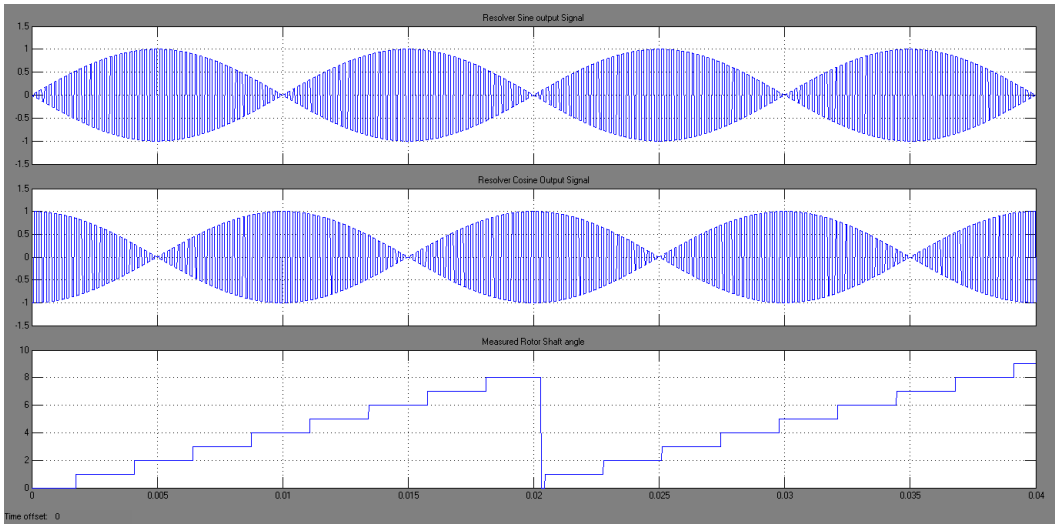

Fig: 3.23 Sine, Cosine modulated signals of resolver and measured rotor shaft angle

4.5 CONCLUSION

To evaluate the performance of the implemented ATO based RDC model, several simulations were carried out for different rotor speeds with constant excitation source of 1 Volt amplitude and a frequency of 5 kHz. From case (i), it can be observed that the performance of the proposed model is good. Whereas from case (iii), it is noticed

that it exhibits pulsating rotor shaft angle estimation even though it is a closed loop model.

From case (i) to case (iii), it can be concluded that ATO based RDC model gives better rotor angle results at lower speeds and the resolution need to be increased at higher speeds. So, the proposed ATO based RDC model not to robust to different speeds and the resolution of this algorithm need to be increased. To improve the robustness and resolution, a modified ATO algorithm is discussed, implemented and experimentally verified in the next chapters.